PAPER

MCNP Dose evaluation around D-D and D-T neutron generators and shielding design

Published by IOP Publishing for Sissa Medialab

Received: *January 31, 2021*
Revised: *August 1, 2021*
Accepted: *September 7, 2021*
Published: *October 1, 2021*

MCNP Dose evaluation around D-D and D-T neutron generators and shielding design

H. Jarahi,[a] **T. Akbarzadeh Chiniforoush**[b] **and Y. Kasesaz**[c,*]

[a] *Department of Physics, K.N. Toosi University of Technology, Tehran, Iran*
[b] *Department of Medical Radiation Engineering, Science and Research Branch, Islamic Azad University, Tehran, Iran*
[c] *Nuclear Science and Technology Research Institute (NSTRI), Tehran, Iran*

E-mail: ykasesaz@aeoi.org.ir

Abstract: In recent years, neutron generators have extensively used as neutron sources and vast efforts have been made to develop high yield neutron generators, so the aspect of radiation shielding during the utilization of neutron generators is unavoidable. In this study, dose distribution around the D-D and D-T neutron generator was calculated by using Monte Carlo simulation. Then an effective shielding was designed and different materials with different thicknesses at distinction distances from the generator were examined. Finally, the organs dose was acquired by using ICRP 110 male phantom with and without shielding at different body position relative to generator tube.

The results show that the dose induced by the D-T generator is 500 times greater than the D-D generator and the neutron dose is about 100 times more than gamma dose. The dose is reduced about 20 times by increasing the distance up to 5 m, however, the presence of Borated-Polyethylene with a thickness of 60 cm as most effective shielding reduces the whole-body dose up to 60%. Besides, inserting a layer of Pb to Borated-Polyethylene is effective to attenuate the gamma-rays. The received dose to organs depends on the body direction relative to tube head of neutron generator. In general, the best position of tube placement relative to shielding wall are 90 and 180 degrees for the D-T and D-D generators, respectively, distance between the generator tube head and the phantom is suggested 200 cm and it is recommended that for most dose reduction, the operator stands in the anterior-posterior position relative to generator tube.

Keywords: Dosimetry concepts and apparatus; Models and simulations; Radiation damage evaluation methods; Neutron sources

*Corresponding author.

https://doi.org/10.1088/1748-0221/16/10/P10001

2021 JINST 16 P10001

Contents

2021 JINST 16 P10001

1 Introduction

Neutron Generators (NG) are extensively used in the various industrial applications such as neutron radiography [1, 2], neutron activation analysis [3–5], boron neutron capture therapy [6–8], explosive material detection [9, 10] and material testing [11].

The most important advantages of neutron generators are compact size, safety, on/off switching and easy to be controlled as well as logical cost [12, 13]. The D-T and D-D neutron generators are commercially available [14]. Extensive efforts have been conducted to develop a high yield NG for various applications [5, 15–17]. The yield of the D-T reaction is 50–100 times higher than the D-D reaction also the D-T fusion reaction has the highest cross-section compared with the D-D [14, 18]. The D-T and D-D reactions generate monoenergetic neutrons of 14 MeV and 2.4 MeV, respectively [19].

Figure 1 shows the neutron yield as a function of deuteron energy for D-T and D-D neutron generators. According to the yield curves in figure 1, the neutron yield of D-T and D-D generators at deuteron energy of 200 keV is 1.45E11$n/(\mathrm{mA}\cdot\mathrm{s})$ and 8E9$n/(\mathrm{mA}\cdot\mathrm{s})$, respectively [14].

The neutron yield and angular distribution of the neutrons as well as the neutron energy at different angles are considerable parameters of generated neutrons. The neutron energy vs. angular distribution of the neutrons (θ) at the deuteron energy (E_d) below 500 keV can be calculated by the eq. (1.1) for the D-D and D-T reactions.

$$E_n\left(E_d,\theta\right) = E_0 + \sum_{i=1}^{n} E_i\left(\cos\theta\right)^i \tag{1.1}$$

Where E_n is the neutron energy, E_0, E_i depend on deuteron energies, which are summarized in table 1. The definition of angles division around the generated tube used in the simulations is represented in figure 2 [14, 20].

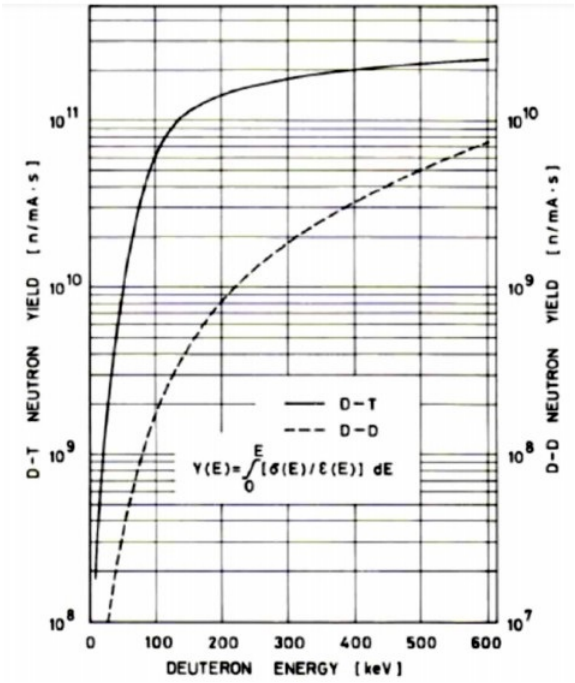

Figure 1. Total neutron yields for D-T and D-D reactions as a function of deuteron energy [14].

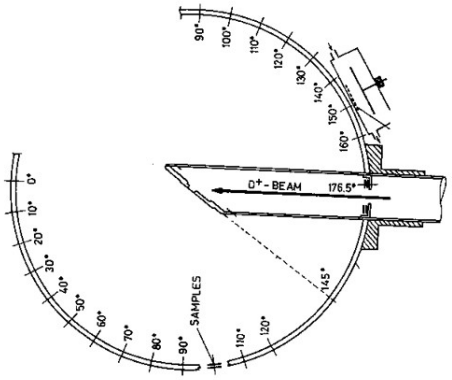

Figure 2. Schematic view of angles division around the generator tube used in the simulations.

Table 1. Values of E_i in eq. (1.1) for the calculation of thin target neutron energy vs. emission angle in the laboratory system [14].

	D-T			D-D			
E_d (keV)	E_0	E_1	E_2	E_0	E_1	E_2	E_3
50	14.04814	0.47679	0.00834	2.46073	0.24848	0.01282	0.00031
100	14.06732	0.67488	0.01719	2.47303	0.35237	0.02524	0.00062
200	14.10711	0.95596	0.03320	2.49771	0.50072	0.05044	0.00242
300	14.14704	1.17282	0.04923	2.52289	0.61581	0.75300	0.00589

2021 JINST 16 P10001

In addition, the angular distributions of the emitted neutrons relative to those of 90 degrees can be calculated by eq. (1.2) for the D-D and D-T reaction.

$$R_n\left(E_d,\theta\right)=\frac{Y\left(\theta\right)}{Y\left(90\right)}=1+\sum_{i=1}^{n}A_i\left(cos\theta\right)^i \tag{1.2}$$

Where $R_n\left(E_d,\theta\right)$ is the neutron yield related to the deuteron energy and the angular distribution of the neutrons, $Y(\theta)$ is the yield of the neutron at θ degrees, and $Y(90)$ is the yield of the neutron at 90 degrees as well as A_i is a coefficient depends on different deuteron energies, which is given in table 2 [14, 20].

Table 2. Recommended value of A_i for calculation of thin target angular distributions of D-T and D-D source yield in laboratory system normalized to 90° [14].

	D-T		D-D				
E_d (keV)	A_1	A_2	A_1	A_2	A_3	A_4	A_5
50	0.03440	0.00110	0.11787	0.58355	−0.11353	0.04222	0.16359
100	0.04820	0.00110	0.01741	0.88746	0.22497	0.08183	0.37225
200	0.06780	0.00050	−0.03149	1.11225	0.38659	0.26676	0.11518
300	0.08180	0.00050	−0.10702	1.64553	0.63645	0.67655	0.35367

The neutron yield and neutron energy for the D-D and D-T neutron generators are shown in figure 3 according to eq. (1.1) and eq. (1.2) [14, 20].

Obviously, vast applications of the high yield neutron generators require the dose evaluations around the neutron generator, and shield design surrounding the generator. Since, the D-D and D-T neutron generators are more common, the aim of this study is to dose evaluation around the D-D and D-T neutron generators as well as organ dose calculation and effective shielding design.

2 Method and materials

All simulations were performed by using Monte Carlo N-Particle code (MCNP, Version 4C, National Laboratory, Los Alamos NM, U.S.A.) [21]. It should be noted that the deuteron energy is assumed 200 keV at all simulations. First, the dose distribution was acquired, then an effective shielding was designed. Finally, organ doses were obtained with and without shielding.

2.1 First simulation study

At first simulation study, a neutron generator tube was simulated in the shape of cylinder shell by 304 stainless steel with the length of 98 cm, inner and outer diameter of 4.75, and 5 cm, respectively. Both sides of the cylinder shell are closed by using two solid cylinders (304 stainless steel) with a diameter and thickness of 6 cm and 1 cm, respectively. The generator tube is symmetric relative to the central axis of the cylinder shell. The neutron generator was assumed above the concrete ground with the thickness of 30 cm at the height of 150 cm.

Dose calculations were performed using the flux-to-dose conversion factors in different spheres around the neutron generator based on the ANSI-1991 standard [22].

2021 JINST 16 P10001

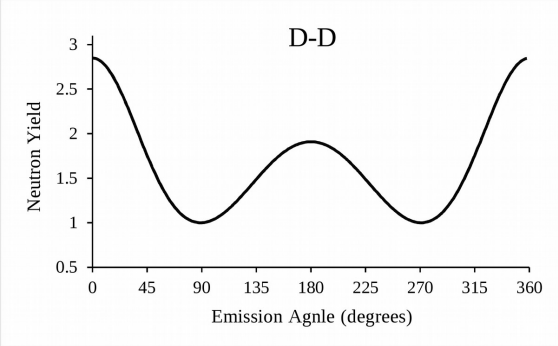

(A) The neutron yield of the D-D neutron generator

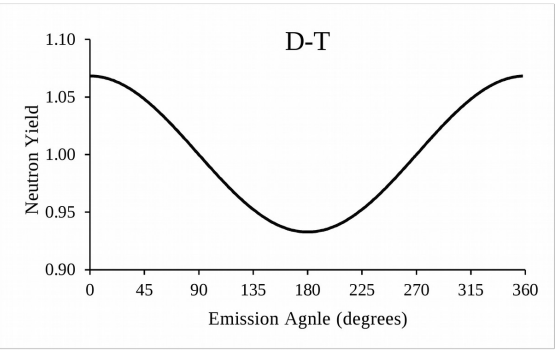

(B) The neutron yield of the D-T neutron generator

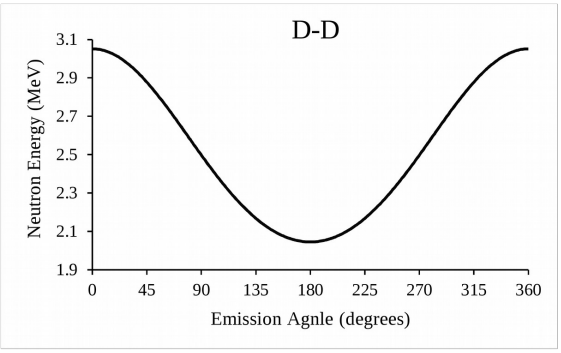

(C) The neutron energy of D-D neutron generator

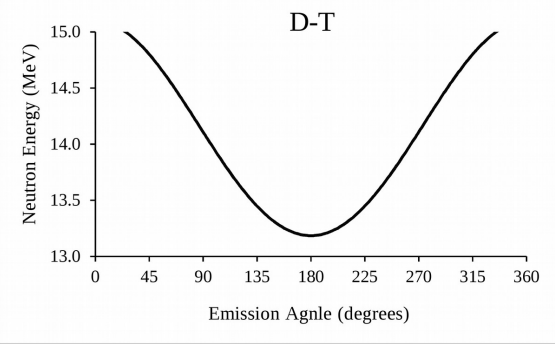

(D) The neutron energy of D-T neutron generator

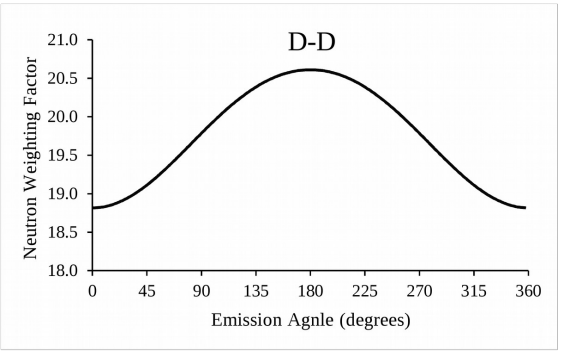

(E) The neutron weighting factor obtained for the D-D neutron generator according eq. (2.3)

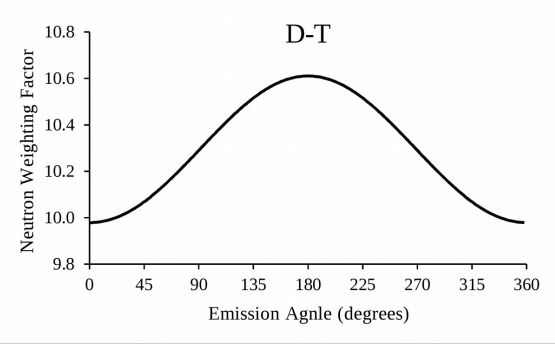

(F) The neutron weighting factor obtained for the D-T neutron generator according eq. (2.3)

Figure 3. A, B) The neutron yield vs. emission angles according to eq. (1.2) for the D-D and D-T neutron generator. C, D) The neutron energy vs. emission angles according to eq. (1.1) for the D-D and D-T neutron generator. E, F) The neutron weighting factor vs. emission angles according to eq. (2.3) and eq. (1.1) for the D-D and D-T. Neutron generator at the deuteron energy of 200 keV [14, 20].

2021 JINST 16 P10001

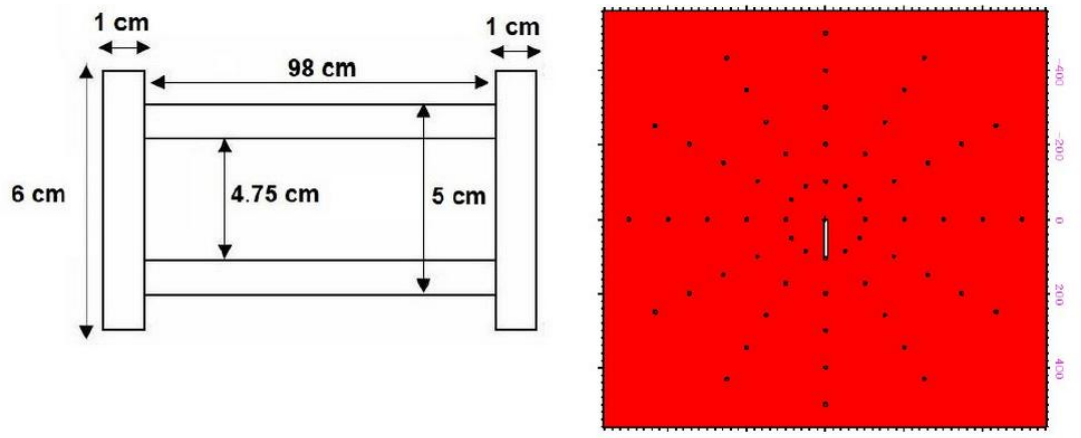

(A) (B)

Figure 4. Simulated geometry including the neutron generator tube and different spheres for dose calculations. A) the dimensions of the generator tube. B) the generator tube was assumed at the center of different spheres for dose calculations.

In addition, the dose rate obtained by simulation was validated by eq. (2.1) around an isotropic point source.

$$D\ (\text{mrem/h}) = \frac{f \cdot S}{4\pi r^2} \tag{2.1}$$

Where D is dose rate, f is flux to the dose conversion factor, S is source flux and r is the distance from the source.

2.2 Second simulation study

It is necessary to make a safe place and also design an effective radiation shielding for operators. Neutron and gamma emissions were considered to design the effective shielding in this work.

Vast varieties of shielding geometries can be considered around the neutron generator, however, the purpose of this work is to find the best effective shielding material and thickness with comparison. Therefore, a simple geometry was considered as much as possible in the shape of a single wall (open geometry).

The shielding was designed as a single wall in length, width, and height of 150, 60, and 200 cm, respectively, which is placed on the concrete ground with the thickness of 30 cm without a ceiling. Dose calculations were assessed by using an air sphere with a radius of 5 cm. The air sphere was supposed tangential to the shielding wall, as well as the distance between the center of the air phantom and the head of the generator tube was assumed 200 cm and the central axis of the tube is perpendicular to the central axis of the body phantom. Different materials were considered including Solid-Boric-Acid (SBA), Polyethylene Non-Borated (PNB), Paraffine (P), Concrete 806 (C), Borated-Polyethylene (60% polyethylene + 30% natural boron) (BP), AlF3 [23]. All shielding materials were examined with different thicknesses of 10, 20, 30, 40, 50, 60 cm at 90 degrees. Additionally, the distance between generator tube and shielding wall were verified at 10 to 70 cm per 10 cm. Finally, a layer of Pb with thickness of 2 cm was inserted to Borated-Polyethylene with thickness of 10 cm to improve the shielding efficiency.

2021 JINST 16 P10001

The gamma flux and the total neutron flux was acquired by using F4 tally (flux tally, unit: particles/cm^2), also the effective dose of gamma and neutron were according to ICRP-21 [24].

2.3 Third simulation study

At the end, the dose evaluation was conducted for an operator who receives unwanted radiation by using ICRP 110 voxel phantom with and without the Borated-Polyethylene shielding with the thickness of 60 cm as the most effective shielding.

In this study, 20 different cases were investigated including different positions of operator's body relative to the head of neutron generator were considered including straight to the generator (anterior-posterior), back to the generator (posterior-anterior), from left to right (lateral-proximal) and from right to left (proximal-lateral), as well as three different angles relative to the deuteron direction including zero, 90 and 180 degrees were simulated with shielding for both the D-D and D-T neutron generators, separately. The 8 and 12 cases for the distance (between the tube head and the phantom) of 150 and 200 cm, respectively. Figure 5 is merely shown the difference in angles between the tube head relative to the operator's body and the different directions of the body. The distance between the phantom center and the center of generator head was assumed 150 and 200 cm and it was supposed that the phantom is tangential to shielding wall. It should be mentioned that dose evaluation was not calculated at 180 degrees at distance (between the tube head and the phantom) of 150 cm, because of the generator size. The center of the tube head was considered as reference point in all calculations. The positions of the generator tube and dimensions is presented in figure 5, in the case that the distance between the tube head and phantom is assumed 200 cm.

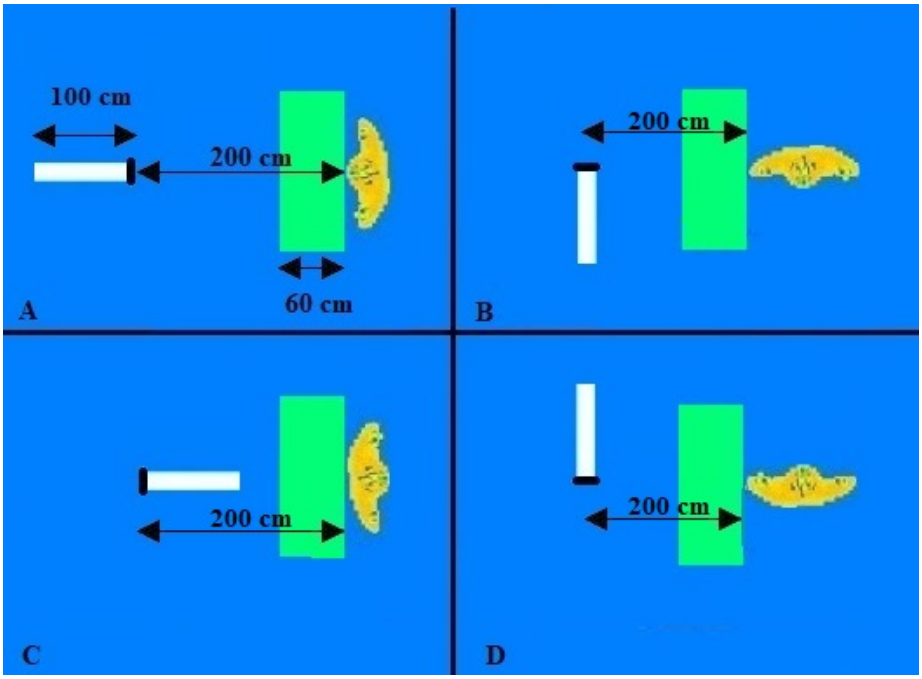

Figure 5. Different positions of operator body relative to the neutron generator. A) anterior-posterior at zero degree. B) proximal-lateral at 90 degrees. C) posterior-anterior at 180 degrees. D) lateral-proximal at 270 degrees.

2021 JINST 16 P10001

Table 3. Recommended tissue weighting factors [25, 26].

Tissue	w_T
Bone-marrow (red), Colon, Lung, Stomach, Breast, Remainder Tissues*	0.12
Gonads	0.08
Bladder, Oesophagus, Liver, Thyroid	0.04
Bone surface, Brain, Salivary glands, Skin	0.01

*Remainder tissues: Adrenals, Extrathoracic (ET) region, Gall bladder, Heart, Kidneys, Lymphatic nodes, Muscle, Oral mucosa, Pancreas, Prostate, Small intestine, Spleen, Thymus, Uterus/cervix.

Organ doses were acquired with and without the Borated-Polyethylene shielding with a thickness, length, height of 60, 150 and 200 cm as most effective shielding.

The total dose due to neutron and gamma was obtained according to ICRP103 for 27 different organs [25]. The neutron dose component is due to the interactions of $^{1}\mathrm{H}(n,n)^{1}\mathrm{H}$ and $^{14}\mathrm{N}(n,p)^{14}\mathrm{C}$ and the gamma dose component is due to the gamma existed in the neutron beam and the interaction of $^{1}\mathrm{H}(n,\gamma)^{2}\mathrm{H}$. The equivalent dose was obtained for each organ by using F6 tally (energy deposition averaged over a cell (MeV/g)) according to eq. (2.2) [25].

$$H_T = \sum_R w_R \cdot D_{T.R} \tag{2.2}$$

Where $D_{T.R}$ is the mean absorbed dose from radiation of type R in a tissue or organ T, and w_R is radiation weighting factor [25], which for gamma at all energies is supposed one, while the neutron weighting factor is applied by using DE6 and DF6 cards in the code input according to eq. (2.3) [25, 26].

$$w_r = \begin{cases} 2.5 + 18.2e^{-[\ln(E_n)]^2/6}, & E_n < 1\,\mathrm{MeV} \\ 5.0 + 17.0e^{-[\ln(2E_n)]^2/6}, & 1\,\mathrm{MeV} \le E_n < 50\,\mathrm{MeV} \end{cases} \tag{2.3}$$

Additionally, the effective dose was calculated by eq. (2.4) [25, 26].

$$E = \sum_T w_T H_T \tag{2.4}$$

Where H_T is the equivalent dose in a tissue or organ T, and w_T is the tissue weighting factor, the recommended tissue weighting factors are given in table 3 [25, 26].

3 Results

The total number of primary particles was adjusted 10E12 in the simulation. With this number of particles, the overall statistical uncertainly is less than 5%.

3.1 Dose distribution (first simulation study)

The spatial dose distribution at different distances of the center of tube head including 1, 2, 3, 4, and 5 m for the D-D and D-T is shown in figure 6. As can be seen in figure 6, the maximum dose

2021 JINST 16 P10001

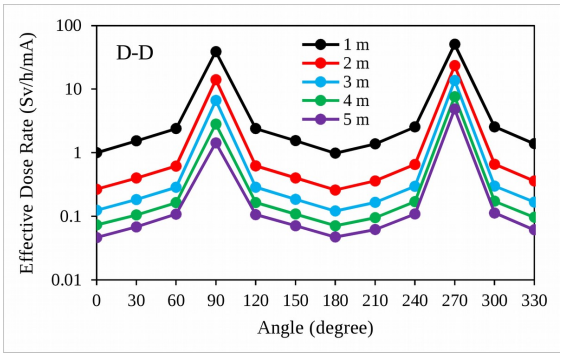

(A) The D-D neutron generator

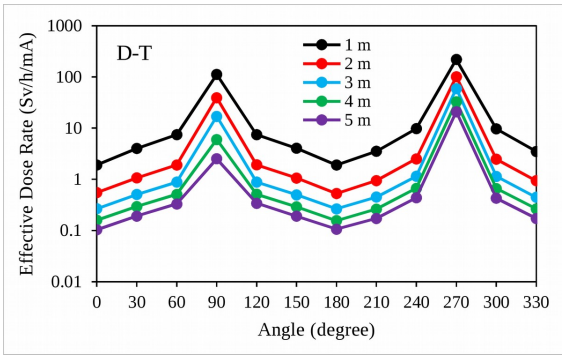

(B) The D-T neutron generator

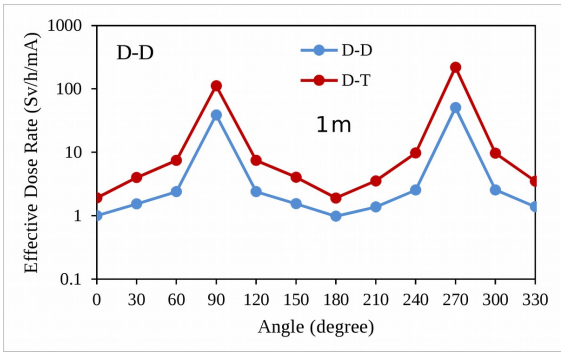

(C) Comparison of the D-D and D-T at distance of 1 m

Figure 6. Spatial dose distribution at different distances of the center of the tube head including 1, 2, 3, 4, and 5 m around A) the D-T neutron generator, and B) The D-D neutron generator. C) The comparison of spatial dose distribution for the D-D and D-T at distance of 1 m of the tube head (refer to figure 4B to see the geometry of this simulation).

rate takes place at 90 and 270 degrees, as well as the minimum dose rate takes place at 180 degrees (end of the tube) for both the D-D and D-T neutron generator.

As expected, the dose rate of the D-T is about 100 times greater than the D-D generator (figure 7). Figure 7 shows the effective dose rate at different distances of the center of the tube head (reference point) including 1, 2, 3, 4 and 5 m at zero degree. As can be seen, by increasing the distance from the head of the generator tube, the effective dose rate reduces, as at distance of 5 m from the tube head, the effective dose rate reduces dramatically.

To validate simulations, the neutron dose was estimated using eq. (2.1) around an isotropic point source. According to eq. (2.1), dose at the distance of 150 cm from the point source with a flux of 10E8(n/s) was obtained 130 (mrem/h), which f is 0.168(mrem/h)$/(n/\mathrm{cm}^2 \cdot \mathrm{s})$. The dose obtained from the MCNP calculation is 134 $(mrem/h)$, which indicates the acceptable accuracy of the calculations.

3.2 Shielding design (second simulation study)

One of the ways to reduce the dose is to increase the distance, however, for the places where there is not enough space, an effective shielding should be designed. Figure 8 and figure 9 shows the gamma

2021 JINST 16 P10001

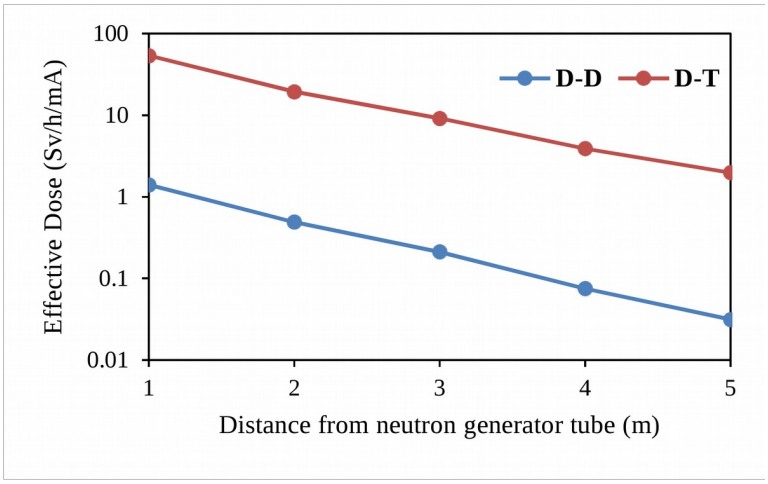

Figure 7. The effective dose rate at different distances from the tube head including 1, 2, 3, 4 and 5 m without shielding wall. The blue and red curves show the effective dose rate around the D-D and D-T neutron generators, respectively. The related geometry is presented in figure 4B.

flux, thermal, epithermal, fast, and total neutron flux, as well as the effective dose of gamma and neutron at the presence of six different materials of shielding including Solid-Boric-Acid (SBA), Polyethylene Non-Borated (PNB), Paraffine (P), Concrete 806 (C), Borated-Polyethylene (BP) and AlF3 with the thicknesses of 10, 20, 30, 40, 50, and 60 cm at 90 degrees for the D-D and D-T neutron generators, respectively. The distance between the center of the air phantom and the head of the generator tube was assumed 200 cm and the air sphere is tangential to the shielding.

As can be seen in figure 8 and figure 9, the neutron dose is approximately 100 times more than the gamma dose, so the most effective shielding should be attenuation of the neutron. The minimum epithermal neutron flux was calculated in presence of Borated-Polyethylene with a thickness of 60 cm for the D-D and D-T. The minimal fast neutron flux was calculated in presence of Paraffine and Borated-Polyethylene with the thickness of 60 cm for the D-D and D-T, respectively. As well as the minimum total neutron flux and neutron dose was obtained in presence of Borated-Polyethylene with a thickness of 60 cm for the D-D and D-T. Above all, the most effective shielding for the D-D and D-T neutron generators is Borated-Polyethylene with a thickness of 60 cm. For the D-D and D-T, the lowest neutron dose in the presence of Borated-Polyethylene with the thickness of 60 cm was obtained 2.585×10^{-13} Sv/h/per particle and $2.243 \times 10^{-13} S$ v/h/per particle, respectively, also the minimum gamma dose the for D-D and D-T was obtained 2×10^{-15} Sv/h/per particle and 15.816×10^{-15} Sv/h/per particle, respectively.

In figure 8 and figure 9, the gamma flux and gamma dose increase dramatically for all shielding materials at the thickness of 10 cm, so a layer of Pb with thickness of 2 cm was inserted to Borated-Polyethylene shielding with different thickness of 10, 20, 30, 40, 50 and 60 cm. As can be seen in figure 10, inserting the layer of Pb to the Borated-Polyethylene affects positively on the gamma dose reduction.

To survey the distance from the neutron tube, different distances of 0, 10, 20, 30, 40, 50, 60, and 70 cm were considered in the presence of Borated-Polyethylene with the thickness of 60 cm as best shielding. As can be seen in figure 11, distance has no effect on the gamma dose and gamma

2021 JINST 16 P10001

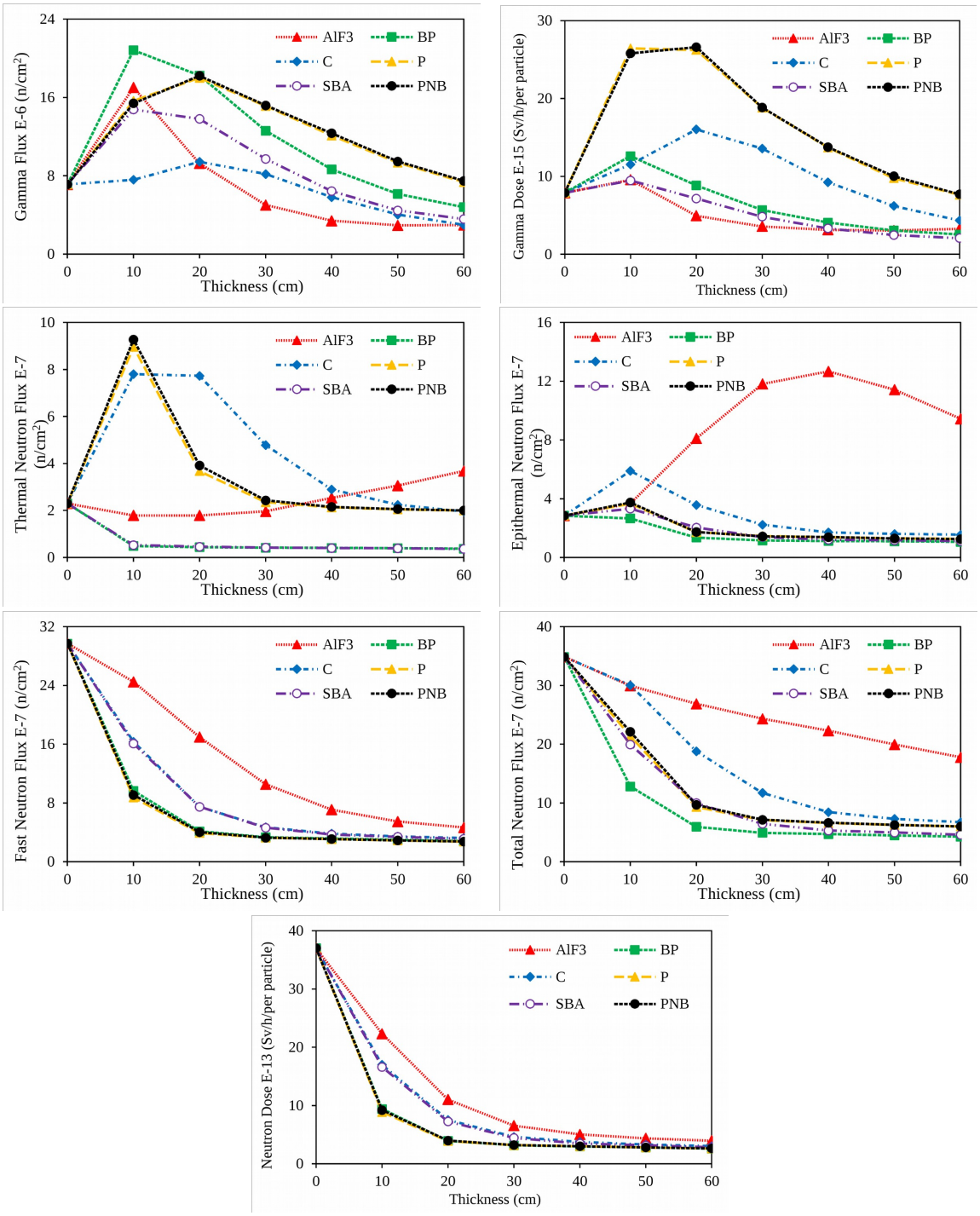

Figure 8. Gamma flux and gamma dose as well as neutron flux and neutron dose in presence of 6 different materials of shielding according to the different thicknesses of 10, 20, 30, 40, 50, and 60 cm at 90 degrees for D-D neutron generator. The distance between the air sphere and the tube head is 200 cm and the air sphere is tangential to the shielding.

2021 JINST 16 P10001

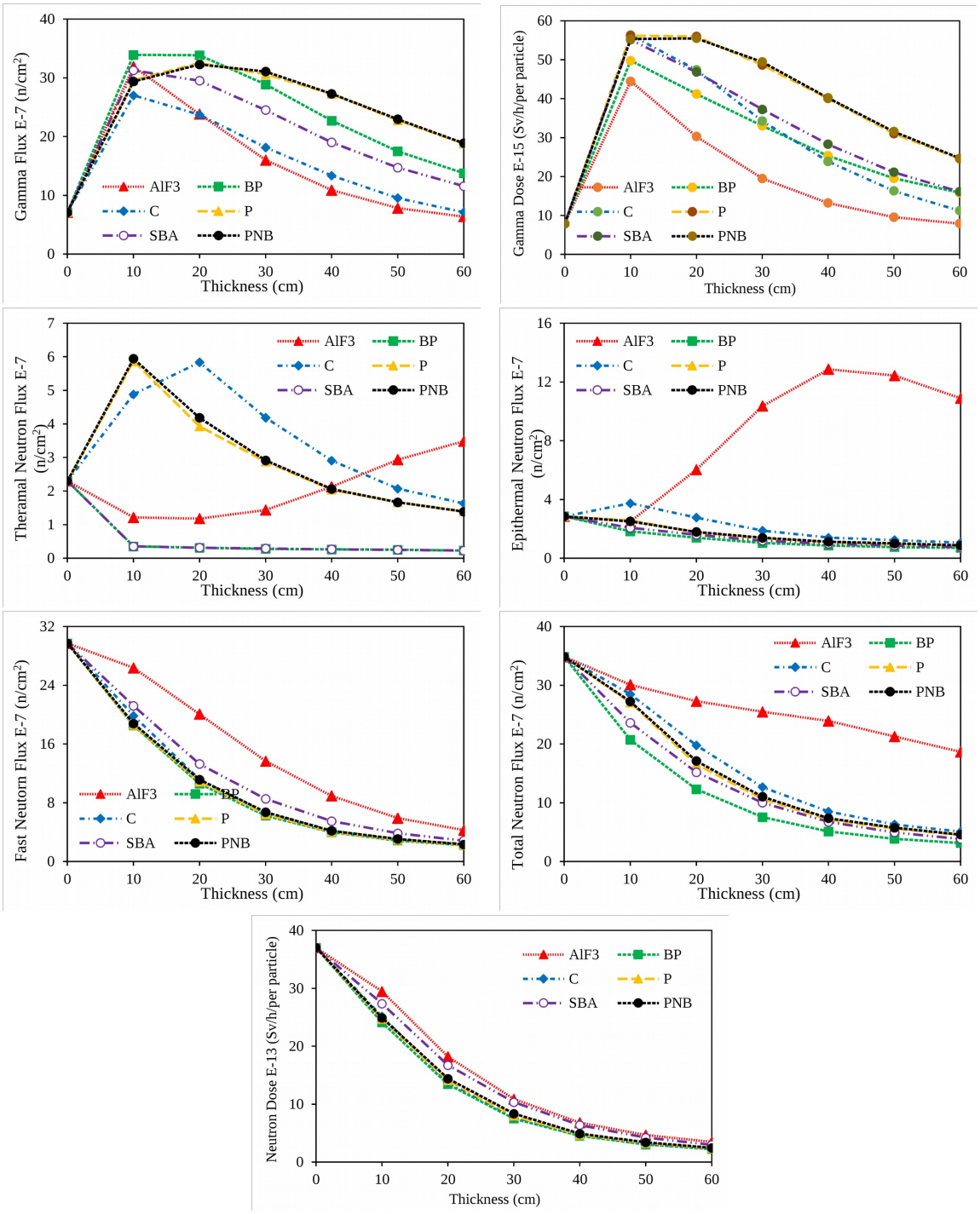

Figure 9. Gamma flux and gamma dose as well as neutron flux and neutron dose in presence of 6 different materials of shielding according to the different thicknesses of 10, 20, 30, 40, 50, and 60 cm at 90 degrees for D-T neutron generator. The distance between the air sphere and the tube head is 200 cm and the air sphere is tangential to the shielding.

2021 JINST 16 P10001

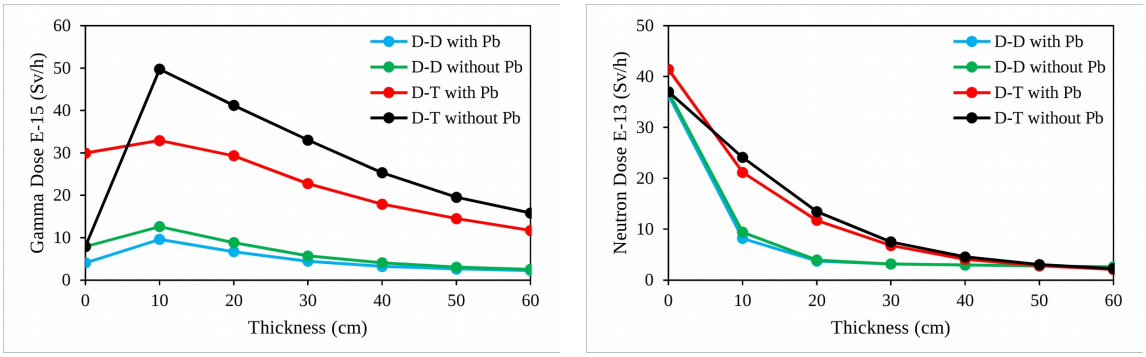

Figure 10. Gamma dose and neutron dose at different thickness of Borated-Polyethylene with and without Pb layer.

flux, however, it does affect on the neutron dose and neutron flux. It should be noted that at the initial examination of the shielding design were performed by using the air spherical phantom.

3.3 Organ doses (third simulation study)

The absorbed dose rate of gamma and neutron as well as total dose for different organs/tissues including lung, stomach, colon, bone marrow (red), breast, reminder, gonads, thyroid, esophagus, bladder, liver, bone surface, skin, brain and salivary glands are given in table 4 and table 5 at distance (between tube head and phantom) 150 cm when the operator direction is anterior-posterior for the D-D and D-T, respectively.

In the direction of anterior-posterior for the D-D generator at distance (between tube head and phantom) of 150 cm, all organs/tissues receive the lowest dose at zero and 90 degrees, with and without shielding, respectively. while, for the D-T is 90 degrees. The maximum dose rate with and without shielding at distance (between tube head and phantom) of 150 cm is received by thyroid and skin.

The equivalent dose and absorbed dose of gamma are equal because the radiation weighting factor of gamma is the constant coefficient of 1 based on ICRP-103 [25]. The equivalent dose rate of neutron and total dose rate (gamma dose and neutron dose) for all the body's organs for the D-D and D-T at distance (between tube head and phantom) of 150 cm are given in table 6 and table 7, respectively.

As well as organs dose was obtained for four different body directions at three different angles relative to the tube head (0, 90, 180 degrees) at distance (between tube head and phantom) of 200 cm (table 8 and table 9). In the matter of absorbed dose at distance (between tube head and phantom) of 200 cm for the D-D generator, at zero, 90 and 180 degrees, the best direction of the operator body is facing the tube, while for the D-T at 180 degrees is the worst angle relative to generator tube.

The effective dose rate of whole body is reported in table 10 for the D-D and D-T neutron generators in presence of Borated-Polyethylene with the thickness of 60 cm. The presence of Borated-Polyethylene with the thickness of 60 cm as shielding reduces the effective dose of whole-body by 96%. As can be seen in table 10 and table 11, the effective dose rate of whole-body for the D-T is remarkably more than D-D generator as well as the effective dose rate reduces by increasing the distance between the center of the tube head and phantom, however, there are exceptions. In

2021 JINST 16 P10001

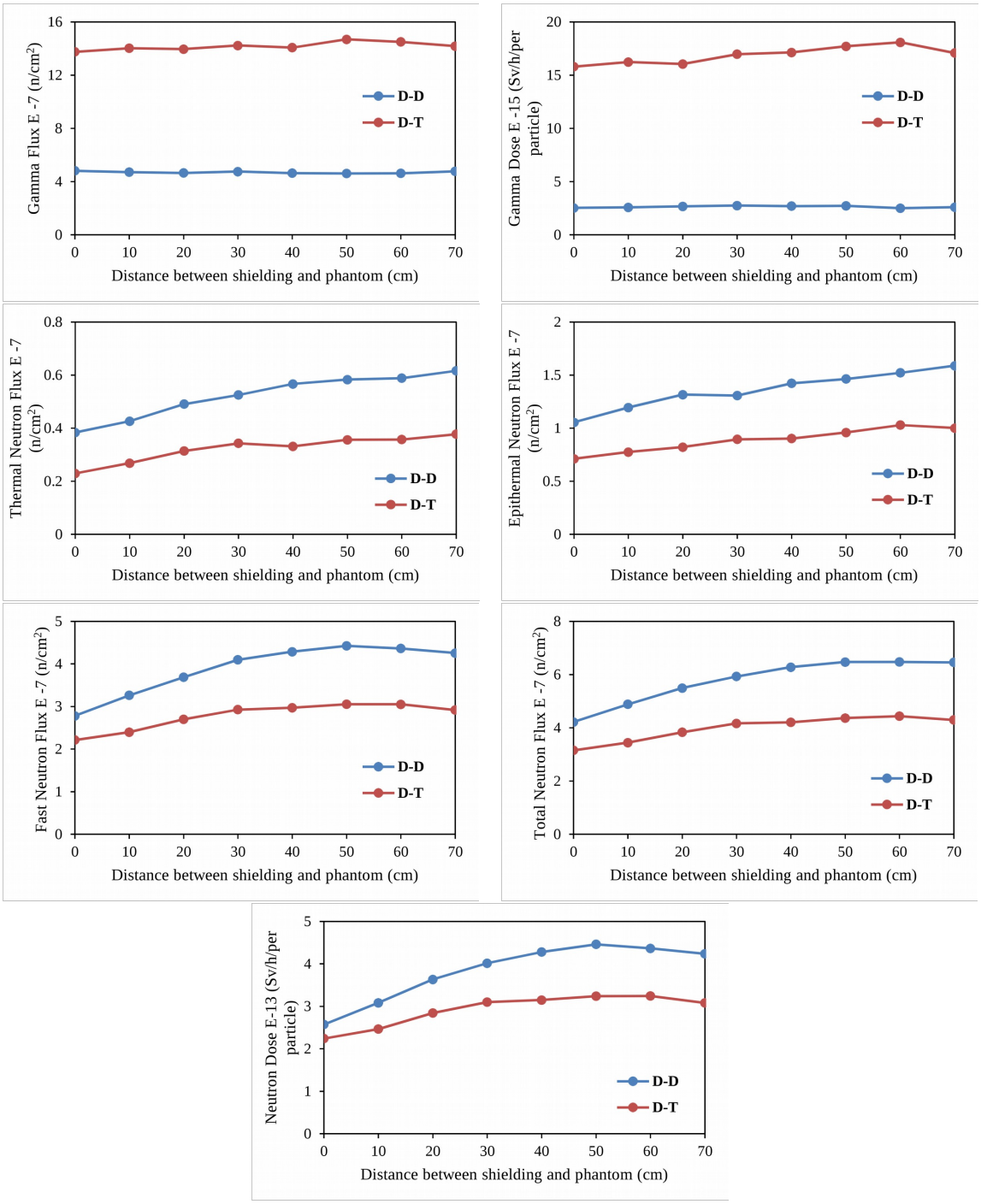

Figure 11. Gamma flux and gamma dose as well as neutron flux and neutron dose in presence of Borated-Polyethylene with the thickness of 60 cm at different distances from the neutron tube including 0, 10, 20, 30, 40, 50, 60 and 70 cm for the D-D and D-T neutron generator.

Table 4. The absorbed dose rate (Gy/s) for body organs (anterior-posterior) at distance (between tube head and phantom) of 150 cm from tube of the D-D neutron generator.

Organ	Gamma absorbed dose rate				Neutron absorbed dose rate				Total absorbed dose rate			
	Without shielding		with shielding		Without shielding		with shielding		Without shielding		with shielding	
	0	90	0	90	0	90	0	90	0	90	0	90
Lung	8.14E−5	7.90E−6	9.25E−7	8.66E−7	5.24E−4	2.27E−5	3.97E−7	5.10E−7	6.05E−4	3.06E−5	1.32E−6	1.38E−6
Stomach	5.35E−5	9.03E−6	8.66E−7	7.91E−7	3.09E−4	3.48E−5	2.37E−7	3.44E−7	3.63E−4	4.38E−5	1.10E−6	1.13E−6
Colon	3.17E−5	7.54E−6	7.97E−7	8.00E−7	2.02E−4	2.79E−5	3.81E−7	6.18E−7	2.34E−4	3.54E−5	1.18E−6	1.42E−6
Bone marrow (red)	3.82E−5	6.31E−6	8.18E−7	8.20E−7	3.20E−4	1.91E−5	6.70E−7	8.81E−7	3.58E−4	2.54E−5	1.49E−6	1.70E−6
Breast	3.28E−5	5.45E−6	1.02E−6	7.40E−7	7.48E−4	7.32E−5	1.15E−6	1.54E−6	7.81E−4	7.86E−5	2.17E−6	2.28E−6
Reminder	4.33E−5	7.27E−6	7.58E−7	8.69E−7	9.33E−5	9.22E−6	3.56E−7	4.86E−7	1.37E−4	1.65E−5	1.11E−6	1.35E−6
Gonads	1.48E−5	6.03E−6	6.53E−7	7.16E−7	1.39E−4	3.46E−5	1.75E−7	2.90E−7	1.53E−4	4.06E−5	8.28E−7	1.01E−6
Thyroid	9.28E−5	5.95E−6	1.09E−6	8.01E−7	5.50E−3	5.26E−5	6.44E−7	8.80E−7	5.60E−3	5.86E−5	1.73E−6	1.68E−6
Esophagus	9.72E−5	7.92E−6	8.99E−7	8.28E−7	1.62E−3	2.63E−5	3.21E−7	4.25E−7	1.72E−3	3.43E−5	1.22E−6	1.25E−6
Bladder	2.56E−5	7.85E−6	6.74E−7	7.53E−7	1.36E−4	2.29E−5	1.10E−7	1.77E−7	1.62E−4	3.08E−5	7.84E−7	9.30E−7
Liver	5.11E−5	7.46E−6	8.34E−7	8.06E−7	2.49E−4	1.86E−5	3.11E−7	5.62E−7	3.00E−4	2.60E−5	1.15E−6	1.37E−6
Bone surface	2.65E−5	5.50E−6	7.25E−7	7.78E−7	2.28E−4	2.11E−5	7.13E−7	1.05E−6	2.54E−4	2.66E−5	1.44E−6	1.83E−6
Skin	1.47E−5	3.97E−6	6.67E−7	6.77E−7	2.59E−4	3.57E−5	1.64E−6	2.38E−6	2.74E−4	3.97E−5	2.31E−6	3.06E−6
Brain	2.73E−5	4.28E−6	9.31E−7	8.85E−7	2.81E−4	2.30E−5	1.80E−6	2.09E−6	3.08E−4	2.73E−5	2.73E−6	2.98E−6
Salivary glands	3.75E−5	4.31E−6	9.27E−7	7.76E−7	7.91E−4	3.80E−5	1.57E−6	2.11E−6	8.29E−4	4.23E−5	2.49E−6	2.88E−6

Table 5. The absorbed dose rate (Gy/s) for body organs (anterior-posterior) at distance (between tube head and phantom) of 150 cm from tube of the D-T neutron generator.

Organ	Gamma absorbed dose rate				Neutron absorbed dose rate				Total absorbed dose rate			
	Without shielding		with shielding		Without shielding		with shielding		Without shielding		with shielding	
	0	90	0	90	0	90	0	90	0	90	0	90
Lung	1.57E−2	2.99E−3	1.21E−3	5.59E−4	5.24E−4	2.27E−5	3.97E−7	5.10E−7	1.91E−1	1.73E−2	3.17E−3	8.89E−4
Stomach	1.12E−2	3.37E−3	1.22E−3	5.84E−4	3.09E−4	3.48E−5	2.37E−7	3.44E−7	1.14E−1	2.44E−2	2.78E−3	9.10E−4
Colon	7.90E−3	3.01E−3	1.01E−3	5.45E−4	2.02E−4	2.79E−5	3.81E−7	6.18E−7	7.83E−2	1.84E−2	2.07E−3	8.56E−4
Bone marrow (red)	9.54E−3	2.63E−3	9.42E−4	5.13E−4	3.20E−4	1.91E−5	6.70E−7	8.81E−7	1.17E−1	1.42E−2	2.09E−3	8.24E−4
Breast	9.44E−3	3.12E−3	1.57E−3	6.77E−4	7.48E−4	7.32E−5	1.15E−6	1.54E−6	1.80E−1	2.79E−2	4.77E−3	1.27E−3
Reminder	9.30E−3	2.70E−3	8.91E−4	4.74E−4	9.33E−5	9.22E−6	3.56E−7	4.86E−7	7.16E−2	1.42E−2	1.75E−3	7.11E−4
Gonads	4.92E−3	2.76E−3	7.23E−4	4.78E−4	1.39E−4	3.46E−5	1.75E−7	2.90E−7	4.67E−2	1.76E−2	1.25E−3	6.97E−4
Thyroid	3.21E−2	3.06E−3	1.53E−3	6.37E−4	5.50E−3	5.26E−5	6.44E−7	8.80E−7	1.28E+00	2.38E−2	5.81E−3	1.09E−3
Esophagus	2.15E−2	2.94E−3	1.21E−3	5.51E−4	1.62E−3	2.63E−5	3.21E−7	4.25E−7	4.58E−1	2.03E−2	3.51E−3	8.59E−4
Bladder	6.57E−3	2.94E−3	7.83E−4	4.75E−4	1.36E−4	2.29E−5	1.10E−7	1.77E−7	5.56E−2	1.70E−2	1.38E−3	6.83E−4
Liver	1.08E−2	2.83E−3	1.14E−3	5.37E−4	2.49E−4	1.86E−5	3.11E−7	5.62E−7	1.02E−1	1.35E−2	2.52E−3	8.12E−4
Bone surface	7.17E−3	2.43E−3	7.56E−4	4.60E−4	2.28E−4	2.11E−5	7.13E−7	1.05E−6	8.39E−2	1.38E−2	1.61E−3	7.63E−4
Skin	5.23E−3	2.22E−3	7.67E−4	4.79E−4	2.59E−4	3.57E−5	1.64E−6	2.38E−6	7.71E−2	1.61E−2	1.84E−3	9.60E−4
Brain	8.15E−3	2.25E−3	1.08E−3	5.68E−4	2.81E−4	2.30E−5	1.80E−6	2.09E−6	1.11E−1	1.49E−2	2.84E−3	1.14E−3
Salivary glands	1.22E−2	2.50E−3	1.31E−3	6.04E−4	7.91E−4	3.80E−5	1.57E−6	2.11E−6	2.37E−1	1.97E−2	3.97E−3	1.19E−3

general, it is recommended that the operator should be placed in the position of anterior-posterior at distance (between tube head and operator) of 200 cm. In addition to the tube should be placed at 90 and 180 degrees relative to the shielding wall for D-T and D-D neutron generators, respectively.

4 Conclusion

The dose of the D-T neutron generator is about 500 times higher than the D-D neutron generator. Dose distribution around the generator tube reduces about 20 times by increasing the distance from the Up to 5 m, but the presence of shielding is more efficient. It should be noted that the experimental dose is greater than the calculated dose in this study because the dose of X-rays is not considered.

2021 JINST 16 P10001

Table 6. The equivalent dose rate (Sv/s) for body organs (anterior-posterior) at distance (between tube head and phantom) of 150 cm for the D-D neutron generator.

Organ	Neutron equivalent dose rate				Total equivalent dose rate			
	Without shielding		with shielding		Without shielding		with shielding	
	0	90	0	90	0	90	0	90
Lung	7.74E−3	3.61E−4	6.24E−6	8.09E−6	7.82E−3	3.69E−4	7.16E−6	8.95E−6
Stomach	4.57E−3	5.55E−4	3.78E−6	5.61E−6	4.63E−3	5.64E−4	4.65E−6	6.40E−6
Colon	3.00E−3	4.48E−4	6.17E−6	1.01E−5	3.04E−3	4.55E−4	6.97E−6	1.09E−5
Bone marrow (red)	4.68E−3	3.07E−4	1.10E−5	1.46E−5	4.72E−3	3.13E−4	1.18E−5	1.54E−5
Breast	1.04E−2	1.16E−3	1.93E−5	2.61E−5	1.05E−2	1.17E−3	2.03E−5	2.68E−5
Reminder	1.42E−3	1.47E−4	5.69E−6	7.78E−6	1.47E−3	1.55E−4	6.45E−6	8.65E−6
Gonads	2.06E−3	5.56E−4	2.83E−6	4.78E−6	2.07E−3	5.62E−4	3.48E−6	5.49E−6
Thyroid	7.74E−2	8.39E−4	1.05E−5	1.46E−5	7.75E−2	8.45E−4	1.16E−5	1.54E−5
Esophagus	2.33E−2	4.17E−4	5.07E−6	6.76E−6	2.34E−2	4.25E−4	5.97E−6	7.59E−6
Bladder	2.03E−3	3.67E−4	1.68E−6	2.72E−6	2.06E−3	3.75E−4	2.35E−6	3.48E−6
Liver	3.69E−3	2.97E−4	4.94E−6	8.97E−6	3.74E−3	3.04E−4	5.77E−6	9.77E−6
Bone surface	3.35E−3	3.40E−4	1.17E−5	1.74E−5	3.37E−3	3.46E−4	1.25E−5	1.82E−5
Skin	3.66E−3	5.71E−4	2.75E−5	4.03E−5	3.68E−3	5.75E−4	2.82E−5	4.10E−5
Brain	4.20E−3	3.74E−4	2.97E−5	3.50E−5	4.22E−3	3.78E−4	3.06E−5	3.59E−5
Salivary glands	1.14E−2	6.11E−4	2.61E−5	3.55E−5	1.15E−2	6.16E−4	2.70E−5	3.63E−5

Table 7. The equivalent dose rate (Sv/s) for body organs (anterior-posterior) at distance (between tube head and phantom) of 150 cm for the D-T neutron generator.

Organ	Neutron equivalent dose rate				Total equivalent dose rate			
	Without shielding		with shielding		Without shielding		with shielding	
	0	90	0	90	0	90	0	90
Lung	1.23E+00	1.15E−1	1.73E−2	3.46E−3	1.25E+00	1.18E−1	1.85E−2	4.02E−3
Stomach	7.23E−1	1.60E−1	1.41E−2	3.30E−3	7.34E−1	1.64E−1	1.53E−2	3.88E−3
Colon	4.96E−1	1.22E−1	9.80E−3	3.27E−3	5.04E−1	1.25E−1	1.08E−2	3.81E−3
Bone marrow (red)	7.33E−1	9.31E−2	1.04E−2	3.43E−3	7.43E−1	9.58E−2	1.13E−2	3.94E−3
Breast	1.06E+00	1.92E−1	2.86E−2	6.45E−3	1.06E+00	1.95E−1	3.01E−2	7.12E−3
Reminder	4.73E−1	9.42E−2	8.07E−3	2.65E−3	4.82E−1	9.69E−2	8.96E−3	3.12E−3
Gonads	2.98E−1	1.20E−1	4.86E−3	2.29E−3	3.03E−1	1.23E−1	5.58E−3	2.77E−3
Thyroid	7.33E+00	1.59E−1	3.34E−2	4.69E−3	7.36E+00	1.62E−1	3.49E−2	5.33E−3
Esophagus	2.77E+00	1.33E−1	1.91E−2	3.16E−3	2.80E+00	1.36E−1	2.03E−2	3.71E−3
Bladder	3.56E−1	1.12E−1	5.49E−3	2.09E−3	3.63E−1	1.15E−1	6.27E−3	2.57E−3
Liver	6.51E−1	8.84E−2	1.25E−2	2.89E−3	6.62E−1	9.13E−2	1.36E−2	3.43E−3
Bone surface	5.27E−1	9.17E−2	7.93E−3	3.43E−3	5.34E−1	9.42E−2	8.68E−3	3.89E−3
Skin	4.67E−1	1.11E−1	1.03E−2	5.68E−3	4.72E−1	1.13E−1	1.11E−2	6.16E−3
Brain	7.15E−1	1.01E−1	1.64E−2	6.48E−3	7.23E−1	1.03E−1	1.75E−2	7.05E−3
Salivary glands	1.44E+00	1.33E−1	2.34E−2	6.58E−3	1.45E+00	1.35E−1	2.47E−2	7.18E−3

2021 JINST 16 P10001

Table 8. The equivalent dose rate (Sv/s) of body organs at different directions the D-D neutron generator at distance (between tube head and phantom) of 200 cm the in presence of Borated-Polyethylene with the thickness of 60.

organ	Anterior-posterior			Posterior-anterior			Proximal-lateral			Lateral-proximal		
	0	90	180	0	90	180	0	90	180	0	90	180
Lung	1.19E−6	9.57E−7	8.74E−7	1.55E−6	1.25E−6	1.18E−6	2.07E−6	2.24E−6	1.69E−6	2.07E−6	2.21E−6	1.68E−6
Stomach	7.81E−7	6.93E−7	5.68E−7	1.70E−6	1.53E−6	1.37E−6	1.84E−6	2.06E−6	1.62E−6	1.53E−6	1.60E−6	1.27E−6
Colon	1.14E−6	1.11E−6	9.20E−7	1.90E−6	1.91E−6	1.62E−6	1.83E−6	2.16E−6	1.63E−6	1.74E−6	2.04E−6	1.50E−6
Bone marrow (red)	1.87E−6	1.63E−6	1.56E−6	1.89E−6	1.66E−6	1.59E−6	2.39E−6	2.60E−6	2.09E−6	2.39E−6	2.62E−6	2.10E−6
Breast	3.24E−6	2.92E−6	2.84E−6	7.56E−6	7.52E−6	7.13E−6	5.81E−6	6.53E−6	5.66E−6	5.81E−6	6.23E−6	5.56E−6
Reminder	1.10E−6	1.06E−6	9.08E−7	4.88E−7	2.98E−7	3.25E−7	1.67E−6	2.36E−6	1.44E−6	1.54E−6	1.93E−6	1.14E−6
Gonads	5.69E−7	5.34E−7	4.39E−7	2.50E−6	2.59E−6	2.39E−6	2.71E−6	3.23E−6	2.50E−6	2.51E−6	3.25E−6	2.51E−6
Thyroid	6.16E−7	5.29E−7	4.67E−7	1.12E−6	1.10E−6	9.95E−7	1.14E−6	1.26E−6	1.01E−6	1.16E−6	1.25E−6	9.77E−7
Esophagus	3.20E−7	2.62E−7	2.32E−7	4.28E−7	3.79E−7	3.39E−7	5.62E−7	6.27E−7	4.67E−7	5.52E−7	5.89E−7	4.20E−7
Bladder	1.38E−7	1.33E−7	9.71E−8	3.19E−7	3.11E−7	2.54E−7	4.86E−7	5.87E−7	3.97E−7	4.66E−7	6.02E−7	4.18E−7
Liver	3.18E−7	3.20E−7	2.49E−7	5.12E−7	4.98E−7	4.16E−7	4.56E−7	4.95E−7	3.72E−7	5.88E−7	6.91E−7	5.04E−7
Bone surface	1.66E−7	1.61E−7	1.43E−7	1.69E−7	1.60E−7	1.46E−7	2.02E−7	2.35E−7	1.82E−7	2.03E−7	2.38E−7	1.83E−7
Skin	3.59E−7	3.70E−7	3.39E−7	3.25E−7	3.27E−7	3.05E−7	4.08E−7	4.84E−7	3.97E−7	4.11E−7	4.89E−7	4.00E−7
Brain	3.93E−7	3.18E−7	3.24E−7	3.84E−7	3.10E−7	3.14E−7	3.97E−7	3.68E−7	3.46E−7	4.03E−7	3.68E−7	3.50E−7
Salivary glands	3.56E−7	3.21E−7	2.99E−7	3.95E−7	3.78E−7	3.52E−7	3.62E−7	3.87E−7	3.23E−7	3.57E−7	3.77E−7	3.26E−7

Table 9. The equivalent dose rate (Sv/s) of body organs at different directions the D-T neutron generator at distance (between tube head and phantom) of 200 cm the in presence of Borated-Polyethylene with the thickness of 60.

organ	Anterior-posterior			Posterior-anterior			Proximal-lateral			Lateral-proximal		
	0	90	180	0	90	180	0	90	180	0	90	180
Lung	1.58E−3	3.49E−4	9.65E−4	1.54E−3	3.67E−4	9.48E−4	8.13E−4	5.07E−4	1.09E−3	1.11E−3	5.09E−4	8.04E−4
Stomach	1.33E−3	3.20E−4	8.25E−4	9.17E−4	3.78E−4	6.39E−4	5.95E−4	4.60E−4	7.30E−4	1.18E−3	4.53E−4	8.04E−4
Colon	1.00E−3	3.43E−4	6.94E−4	7.85E−4	3.97E−4	6.21E−4	6.62E−4	4.70E−4	8.23E−4	9.22E−4	4.71E−4	6.90E−4
Bone marrow (red)	1.06E−3	3.74E−4	7.35E−4	1.13E−3	3.75E−4	7.75E−4	7.43E−4	4.93E−4	9.46E−4	9.54E−4	4.99E−4	7.33E−4
Breast	2.55E−3	6.52E−4	1.63E−3	1.18E−3	9.48E−4	1.09E−3	1.44E−3	9.88E−4	1.83E−3	1.85E−3	1.00E−3	1.43E−3
Reminder	8.17E−4	3.14E−4	5.62E−4	1.36E−3	2.90E−4	7.82E−4	5.05E−4	3.94E−4	6.37E−4	9.65E−4	3.77E−4	7.14E−4
Gonads	5.96E−4	2.71E−4	4.51E−4	5.71E−4	4.46E−4	5.21E−4	5.82E−4	5.74E−4	6.37E−4	6.32E−4	5.52E−4	5.86E−4
Thyroid	9.66E−4	1.57E−4	5.10E−4	6.03E−4	1.85E−4	3.75E−4	3.93E−4	2.25E−4	5.88E−4	5.85E−4	2.37E−4	3.75E−4
Esophagus	5.69E−4	1.05E−4	3.31E−4	4.90E−4	1.07E−4	3.08E−4	2.55E−4	1.46E−4	3.52E−4	3.80E−4	1.58E−4	2.58E−4
Bladder	2.05E−4	7.73E−5	1.54E−4	1.75E−4	9.01E−5	1.46E−4	1.62E−4	1.31E−4	1.81E−4	1.85E−4	1.40E−4	1.59E−4
Liver	3.95E−4	9.89E−5	2.57E−4	3.36E−4	1.15E−4	2.35E−4	2.73E−4	1.42E−4	3.81E−4	2.31E−4	1.50E−4	1.89E−4
Bone surface	7.18E−5	3.26E−5	5.35E−5	7.59E−5	3.19E−5	5.55E−5	5.55E−5	4.13E−5	6.73E−5	6.77E−5	4.18E−5	5.51E−5
Skin	9.60E−5	5.37E−5	7.68E−5	9.68E−5	4.92E−5	7.56E−5	8.21E−5	6.51E−5	9.70E−5	9.75E−5	6.58E−5	8.25E−5
Brain	1.38E−4	5.85E−5	1.02E−4	1.46E−4	5.65E−5	1.07E−4	1.12E−4	6.72E−5	1.46E−4	1.44E−4	6.71E−5	1.10E−4
Salivary glands	1.84E−4	5.67E−5	1.22E−4	1.69E−4	6.07E−5	1.17E−4	1.16E−4	6.77E−5	1.60E−4	1.62E−4	6.78E−5	1.16E−4

Table 10. The effective dose rate (Sv/min) of whole-body phantom for the D-D and D-T neutron generator with Borated-Polyethylene with the thickness of 60 cm, the distance between the tube head and phantom are assumed 150 and 200 cm.

Effective Dose Rate	Distance 150 cm		Distance 200 cm		
	0	90	0	90	180
D-D	0.00056	0.00076	0.00075	0.00068	0.00062
D-T	0.94196	0.25705	0.69366	0.19579	0.44838

Table 11. The effective dose rate (Sv/min) of whole-body phantom at different direction of body for the D-D and D-T neutron generator with Borated-Polyethylene with the thickness of 60 cm, the distance between the tube head and phantom is assumed 200 cm.

Effective Dose Rate (Sv/min)		Distance 200 cm		
		0	90	180
D-D	Anterior-posterior	0.00075	0.00068	0.00062
	Posterior-anterior	0.00127	0.00121	0.00112
	Proximal-lateral	0.00134	0.00154	0.00121
	Lateral-proximal	0.00130	0.00147	0.00116
D-T	Anterior-posterior	0.69366	0.19579	0.44838
	Posterior-anterior	0.57437	0.23372	0.40746
	Proximal-lateral	0.40748	0.28637	0.52018
	Lateral-proximal	0.56748	0.28759	0.42658

The neutron dose is approximately 100 times more than the gamma dose, so the most effective shielding should be attenuation of the neutron. Consequently, Borated-Polyethylene was attained as the most effective shielding for the D-D and D-T. The presence of Borated-Polyethylene with the thickness of 60 cm reduces the whole-body dose by 60% more.

To conclude, after analyzing what elaborated above for dose reduction in the presence of Borated-Polyethylene with a thickness of 60 cm as most effective shielding, the best distance between tube head and operator is suggested 200 cm and it is recommended that for dose reduction, the operator is placed in the anterior-posterior position, and the best position of tube placement relative to shielding wall is 90 and 180 degrees with for the D-T and D-D generators, respectively.

References

[1] K. Bergaoui, N. Reguigui, C.K. Gary, J.T. Cremer, J.H. Vainionpaa and M.A. Piestrup, *Design, testing and optimization of a neutron radiography system based on a deuterium-deuterium (D-D) neutron generator*, *J. Radioanal. Nucl. Chem.* **299** (2013) 41.

[2] C.J. Yi and S. Nilsuwankosit, *Development of fast neutron radiography system based on portable neutron generator*, *AIP Conf. Proc.* **1704** (2016) 30007.

[3] N. Marchese, A. Cannuli, M. Caccamo and C. Pace, *New generation non-stationary portable neutron generators for biophysical applications of neutron activation analysis*, *Biochim. Biophys. Acta General Subj.* **1861** (2017) 3661.

[4] F. Mostafaei, S.P. Blake, Y. Liu, D.A. Sowers and L.H. Nie, *Compact DD generator-based neutron activation analysis (NAA) system to determine fluorine in human bonein vivo: a feasibility study*, *Physiol. Meas.* **36** (2015) 2057.

[5] J.H. Vainionpaa, A.X. Chen, M.A. Piestrup, C.K. Gary, G. Jones and R.H. Pantell, *Development of high flux thermal neutron generator for neutron activation analysis*, *Nucl. Instrum. Meth. B* **350** (2015) 88.

[6] M. Hsieh, Y. Liu, F. Mostafaei, J.M. Poulson and L.H. Nie, *A feasibility study of a deuterium-deuterium neutron generator-based boron neutron capture therapy system for treatment of brain tumors*, *Med. Phys.* **44** (2017) 637.

2021 JINST 16 P10001

[7] Y. Kasesaz, H. Khalafi and F. Rahmani, *Optimization of the beam shaping assembly in the D-D neutron generators-based BNCT using the response matrix method*, *Appl. Radiat. Isot.* **82** (2013) 55.

[8] S. Hang, X. Tang, D. Shu, Y. Liu, C. Geng, C. Gong et al., *Monte Carlo study of the beam shaping assembly optimization for providing high epithermal neutron flux for BNCT based on D-T neutron generator*, *J. Radioanal. Nucl. Chem.* **310** (2016) 1289.

[9] V. Bom, M. Ali and C. van Eijk, *Land mine detection with neutron back scattering imaging using a neutron generator*, *IEEE Trans. Nucl. Sci.* **53** (2006) 356.

[10] D.S. Haslip, T. Cousins, H.R. Andrews, J. Chen, E.T.H. Clifford, H. Ing et al., *DT neutron generator as a source for a thermal neutron activation system for confirmatory land mine detection*, in *Hard X-Ray and Gamma-Ray Detector Physics III*, *Proc. SPIE* **4507** (2001) 232.

[11] G.L. Kulcinski, R.F. Radel and A. Davis, *Near term, low cost, 14 MeV fusion neutron irradiation facility for testing the viability of fusion structural materials*, *Fusion Eng. Des.* **109-111** (2016) 1072.

[12] J.G. Fantidis, B.V. Dimitrios, P. Constantinos and V. Nick, *Fast and thermal neutron radiographies based on a compact neutron generator*, *J. Theor. Appl. Phys.* **6** (2012) 20.

[13] K.-N. Leung, J. Reijonen, F. Gicquel, S. Hahto and T.-P. Lou, *Compact neutron generator development and applications*, Ernest Orlando Lawrence Berkeley National Laboratory, Berkeley, CA, U.S.A. (2004).

[14] G.J. Csikai, *CRC handbook of fast neutron generators*, 1987.

[15] V. Skalyga, I. Izotov, S. Golubev, S. Razin, A. Sidorov, A. Maslennikova et al., *Neutron generator for BNCT based on high current ECR ion source with gyrotron plasma heating*, *Appl. Radiat. Isot.* **106** (2015) 29.

[16] C. Waltz, *High-Flux Neutron Generator Facility for Geochronology and Nuclear Physics Research*, 2015APS..APR.S5009W.

[17] X. Lu, J. Wang, Y. Zhang, J. Li, L. Xia, J. Zhang et al., *Design of a high-current low-energy beam transport line for an intense D-T/D-D neutron generator*, *Nucl. Instrum. Meth. A* **811** (2016) 76.

[18] C.E. Moss, W.L. Myers, G.M. Sundby, D.L. Chichester and J.P. Johnson, *Survey of Neutron Generators for Active Interrogation*, Los Alamos National Laboratory (LANL), Los Alamos, NM, U.S.A. (2017).

[19] A. Persaud, O. Waldmann, R. Kapadia, K. Takei, A. Javey and T. Schenkel, *A compact neutron generator using a field ionization source*, *Rev. Sci. Instrum.* **83** (2012) 02B312.

[20] Y. Kasesaz and M. Karimi, *A novel design of beam shaping assembly to use D-T neutron generator for BNCT*, *Appl. Radiat. Isot.* **118** (2016) 317.

[21] J.F. Briesmeister, *MCNPTM-A general Monte Carlo N-particle transport code*, Version 4C, Tech. Rep., LA-13709-M, Los Alamos National Laboratory, (2000).

[22] *Neutron and gamma-ray fluence-to-dose factors*, ANSI/ANS-6.1.1-1991, American Nuclear Society, La Grange Park, IL, U.S.A. (1991).

[23] M. Babaei, A. Sadighzadeh, M. Kiashemshaki, S. Vosoghi, A.A. Zaeem, Y. Kasesaz et al., *Simulation and design of biological shield for the 115 kJ IR-MPF-100 plasma focus device using MCNP code*, *J. Fusion Energy* **35** (2016) 579.

[24] J.B. Massey, *Data for Protection against Ionizing Radiation from External Sources: Supplement to ICRP Publication 15*, Taylor & Francis (1974).

[25] *The 2007 Recommendations of the International Commission on Radiological Protection*, *ICRP publication 103*, *Ann. ICRP* **37** (2007).

[26] J.B. Ludlow, L.E. Davies-Ludlow and S.C. White, *Patient risk related to common dental radiographic examinations*, *J. Am. Dent. Assoc.* **139** (2008) 1237.

2021 JINST 16 P10001